Measurement of electron wave functions and confining potentials via photoemission

A. Mugarza,[1,2] J. E. Ortega,[1,2] F. J. Himpsel,[3] and F. J. García de Abajo[1,4]
[1] *Donostia International Physics Center (DIPC), Aptdo. 1072, 20080 San Sebastián, Spain*
[2] *Departamento de Física Aplicada I, Universidad del País Vasco, Plaza Oñati 2, 20018 San Sebastián Spain*
[3] *Department of Physics, University of Wisconsin Madison*
[4] *Centro Mixto de Materiales CSIC/UPV, Paseo Manuel Lardizabal 3, E-20018 San Sebastian, Spain*
(Dated: February 1, 2008)

Wave functions and electron potentials of laterally-confined surface states are determined experimentally by means of photoemission from stepped Au(111) surfaces. Using an iterative formalism borrowed from x-ray diffraction, we retrieve the real-space wave functions from the Fourier transform of their momentum representations, whose absolute values in turn are directly measured by angle-resolved photoemission. The effective confining potential is then obtained by introducing the wave functions into Schrödinger's equation.

PACS numbers: 79.60.Bm,68.35.Bs,73.21.-b

The electron wave functions and potentials in low-dimensional systems are of primary importance for tailoring electronic properties of nanostructures. The electron energy levels and the probability density are the physical observables. These can be obtained in real space from local conductance maps via scanning tunneling microscopy/spectroscopy (STM/STS) [1, 2], or in reciprocal space by angle-resolved photoemission [3, 4]. The latter has been used to study thin films [3] or two-dimensional arrays of nano-objects [4], whereas STM/STS resolves individual nanostructures on a surface.

The question arises whether it is possible to directly derive wave functions and/or electron potentials from experimental data. The standard procedure consists of assuming a model potential, whose parameters are obtained by fitting the experiment. For instance, in core-level photoelectron diffraction muffin-tin potentials are assumed for retrieving atomic positions that fit the experiment [5, 6]. The electron density of surface states confined between two steps has been measured by STM [1, 2] and has been modeled by semitransparent mirrors located at the step edges [2]. It has been argued that the position of the mirror has to be moved slightly away from the steps to account for electron spill over [7].

We introduce a direct method to determine the effective electron potential from angle-resolved photoemission data, without any a priori knowledge about its nature. All the necessary information is contained in the momentum distribution of the photoemission intensity. This allows us to unambiguously determine the potential and wave functions of one-dimensional quantum well states on stepped Au(111). The real-space wave functions are derived by Fourier transform of their momentum-space representations, the square of which is proportional to the photoelectron intensity under the conditions discussed below. However, the phase in momentum space is not measured and this leads to the well-known phase problem in optics, shared with many other techniques, such as x-ray and electron diffraction [8]. Various iteration methods have been devised to retrieve real-space objects from the modulus of their momentum space representation, in particular the oversampling method [9]. These methods are valid for a confined wave function, because the phase is obtained by repeatedly diminishing the amplitude of the wave function outside the confinement region. The one-electron potential can be obtained after dividing the Schrödinger equation by the wave function.

As a test system we use vicinal noble metal surfaces characterized by equally-spaced, linear step arrays and one-dimensional surface states confined within individual terraces of nominal size L. That is the case of Au(111) vicinal surfaces with relatively wide terraces, such as Au(788) ($L = 38$ Å) and Au(11,12,12) ($L = 56$ Å) shown in Fig. 1 [4, 10]. On Au(11,12,12), the lowest three quantum-well levels ($N = 1 - 3$) lie below the Fermi energy and they can be probed by photoemission, as shown in Figs. 2(a)-(b). The emission angle θ is given relative to the terrace normal in the plane perpendicular to the step array. The data have been taken at the PGM beam line in the Synchrotron Radiation Center (SRC) of the UW-Madison, using a hemispherical Scienta SES200 spectrometer. The energy and angular resolution were 20+7 meV (photons + electrons) and 0.3°, respectively. The light is p-polarized and incident 60° off-normal. By tuning the photon energy to 60 eV we avoid overlap between surface umklapp replicas [10]. Fig. 2(c) shows the angular photoemission intensity scan for each quantum level as obtained from the areas of the peaks in Fig. 2(a). The scale for the component of the photoelectron wave vector parallel to the terrace q_x has been determined from the emission angle and the kinetic energy E as $q_x = \sin\theta\sqrt{2mE}/\hbar$. The parallel momentum scale is shifted by the reciprocal step lattice vector $g = 2\pi/L = 0.11$ Å^{-1} to bring it into the first Brillouin zone [10] and corrected for the small parallel photon momentum of 0.026 Å^{-1}.

The photoemission intensity in reciprocal space $\mathbf{q}$ can be understood in the framework of standard photoemission theory, assuming a one-electron description. We start with the photoemission intensity, which is proportional to the matrix element

$$I_N(\mathbf{q}_\parallel) \propto | < \mathbf{q}|e^{i\mathbf{k}\cdot\mathbf{r}}\mathbf{A}\cdot\nabla|\Psi_N > |^2. \qquad (1)$$

Ψ_N is the initial surface state wave function, $|\mathbf{q}>$ is the final electron state of momentum $\mathbf{q} = (\mathbf{q}_\parallel, q_z)$, $\mathbf{q}_\parallel$ is the momentum component parallel to the surface, $\mathbf{A}$ is the light polarization vector, $\mathbf{k}$ is the momentum of the photon, and N refers to the quantum number of the wave function. To proceed further, it will be assumed that the surface state wave functions can be factorized into components that are either parallel or perpendicular to the surface, i.e. [11]:

$$\Psi_N(\mathbf{r}) = \phi_N(\mathbf{R})\varphi(z),$$

where $\mathbf{R}$ denotes the coordinates along the surface. If, in addition to the surface-state confinement in the perpendicular direction z, the electron is also bound to a 2D region of the surface, the parallel component of the wave function $\phi_N(\mathbf{R})$ must adopt a form which depends on the detailed shape of the confining region and on the boundary conditions at its border. Thus, I_N can be written as

$$I_N(\mathbf{q}_\parallel) \propto \quad C| < \mathbf{q}_\parallel|\phi_N > |^2,$$

where

$$C = | < q_z|\mathrm{e}^{\mathrm{i}k_z z} A_z \frac{\partial}{\partial z}|\varphi > |^2$$

depends very weakly on $\mathbf{q}_\parallel$, so that it can be absorbed into a normalization factor that we set to 1. Therefore, there is a direct relation between photoemission intensity $I_N(\mathbf{q}_\parallel)$ and the Fourier transform of the wave function $\tilde{\phi}_N(\mathbf{q}_\parallel)$:

$$\tilde{\phi}_N(\mathbf{q}_\parallel) =< \mathbf{q}_\parallel|\phi_N >= \int d\mathbf{R}\mathrm{e}^{-\mathrm{i}\mathbf{q}_\parallel\cdot\mathbf{R}}\phi_N(\mathbf{R}). \qquad (2)$$

Thereby we neglect multiple scattering in the final state, which corresponds to Fourier components $\mathbf{q}_\parallel+\mathbf{g}_\parallel$ with a reciprocal lattice vector $\mathbf{g}_\parallel$. These affect the intensity distribution between different Brillouin zones but not the momentum distribution within one Brillouin zone (compare this to the spot profiles in LEED which are not affected by multiple scattering [12]). This permits obtaining the wave function in real space $\phi_N(\mathbf{R})$ from the intensity in reciprocal space as

$$\phi_N(\mathbf{R}) = \int \frac{d\mathbf{q}_\parallel}{(2\pi)^2}\mathrm{e}^{\mathrm{i}\mathbf{q}_\parallel\cdot\mathbf{R}}\sqrt{I_N(\mathbf{q}_\parallel)}\mathrm{e}^{\mathrm{i}\delta_N(\mathbf{q}_\parallel)}. \qquad (3)$$

However, this equation still contains an unknown phase $\delta_N(\mathbf{q}_\parallel)$. We have explored two methods to obtain this phase: (1) an iterative procedure using oversampling [8, 9] and (2) an expansion of the wave function into a Fourier series combined with a least squares fit. In both cases, the strategy is minimizing $|\phi|$ outside the confinement region.

For the iterative method, we begin with a constant phase $\delta_N(\mathbf{q}_\parallel) = 0$ to start the iteration with Eq. (3). The resulting $\phi_N(\mathbf{R})$ is corrected outside the confining region, and transformed back into $\mathbf{q}_\parallel$ space using Eq. (2). The phase of $\tilde{\phi}_N(\mathbf{q}_\parallel)$ is extracted and inserted again into Eq. (3) to start a new iteration. The confinement length is obtained directly from the photoemission data (see below), and the noted correction consists of subtracting from the newly calculated real-space wave function the wave function at the previous step multiplied by a factor 0.1. This ensures convergence to a wave function that vanishes outside the confinement region. As a strong test of convergence of this iterative technique, we have used the phase of the $N = 2$ state to start the iteration of the $N = 1$ state. The first iteration step leads to a wave function that resembles that of the $N = 2$ state, a clear indication of the importance of the phase [8], and convergence to the true $N = 1$ state is achieved after several hundred iterations.

This iterative method leads to results that are in agreement with those derived from an expansion of the wave function into sine functions that vanish at the edges of the confinement region. Moreover, the length of the region where the wave function takes non-negligible values is not sensitive to the input value for the length of the confinement region.

The size of the confining region is obtained from the Fourier transform of the experimental intensity distribution, which can be written as the self-convolution of the real-space wave function,

$$\int \frac{d\mathbf{q}_\parallel}{(2\pi)^2}\,\mathrm{e}^{\mathrm{i}\mathbf{q}_\parallel\cdot\mathbf{R}} I_N(\mathbf{q}_\parallel) = \int d\mathbf{R}'\phi_N(\mathbf{R}')\phi_N^*(\mathbf{R}'-\mathbf{R}). \qquad (4)$$

This convolution takes non-zero values in an area twice the size of the confining region. For the data of Fig. 2 in particular, one obtains curves that are basically confined within a region of $\approx$ 60 Åin diameter (not shown), in agreement with the nominal terrace width in Au(11 12 12), $L = 56$ Å.

The natural normalization for both the two-dimensional wave function ϕ_N and the measured intensity is provided by Eq. (4) if one sets $\mathbf{R} = 0$:

$$\int \frac{d\mathbf{q}_\parallel}{(2\pi)^2} I_N(\mathbf{q}_\parallel) =< \phi_N|\phi_N >= 1.$$

Applying this procedure to the angular scans of Fig. 2(c), we have obtained the surface state wave functions for quantum-well levels in Au(11 12 12) that are shown in Fig. 1. All three wave functions are confined to a region whose width matches the terrace width L. Thus the wave functions exhibit a clear terrace confinement that has not been assumed by our reconstruction procedure, but rather it has emerged from the information contained in the photoemission data.

The actual effective potential of the terrace can be retrieved from the Schrödinger equation as

$$V(\mathbf{R}) - E_N = \frac{\hbar^2}{2m^*\phi_N(\mathbf{R})}\nabla^2\phi_N(\mathbf{R}), \qquad (5)$$

where $m^* = 0.26m$ is the effective mass of the electron in the initial state of energy E_N, taken from the dispersion of the surface state on flat Au(111). The potential becomes independent of the quantum number N if many-electron effects are absent, as we assumed initially.

The experimental wave functions of Fig. 1 have been introduced into Eq. (5) and the resulting electron potential has been represented in Fig. 3. In order to compare the potential derived from the quantum states with various N we add on the left side of Eq. (5) the respective experimental values $E_N^{\rm exp}$ shown in Fig. 1 (horizontal bars). Excellent mutual agreement is obtained for the shape of the potential derived independently from each of the three wave functions $N = 1 - 3$, proving the validity of our method. The potential exhibits a smooth central region and sharp boundaries that force electron confinement. It must be stressed that the validity of Eq. (5) is limited to regions where the wave function is not too small, and therefore, the asymptotic limit of the step barrier potential cannot be determined.

There is a slight uphill/downhill asymmetry of ϕ and V, which is related to an asymmetry of $|\tilde{\phi}|$ for $\pm q$. This effect shows up for the highest level ($N = 3$), which is the least confined. Such an asymmetry explains the asymmetric reflectivity observed in STM [2] where the downhill step reflects more strongly than the uphill. The asymmetry increases for higher-lying empty states which start spilling over the weaker potential barrier on the uphill side.

The same iterative procedure has been applied to the one-dimensional quantum well of Au(788), measured in a different system [4]. In this case the terraces are 38 Åwide and only the first two quantum levels are occupied. We also obtain a good consistency in the electron potential between the two levels. The resulting average is displayed in Fig. 1, and compared with the average potential of Au(11,12,12). In contrast to the latter case, the width of the potential well in Au(788) is narrower than the terrace size, as also observed in thin Pb films [7].

In summary, we have introduced a simple procedure for directly obtaining wave functions and effective potentials of confined electronic states from the momentum distribution of the photoemission intensity. This procedure, which relies on photoemission theory within the one-electron approach, has been successfully tested in the case of laterally confined surface states on Au(111) vicinal surfaces. The method is of general applicability for discrete states because they are spatially confined and allow an iterative determination of the phase by forcing ϕ=0 outside the confinement region. It can be applied to any type of surface nanostructure confined in at least one dimension, such as arrays of quantum wires and quantum dots. While STM provides direct images of the low spatial frequencies, photoemission determines the high spatial frequencies. It would be interesting to pursue the reverse transformation from the real space $|\phi|$ in STM to $\tilde{\phi}$ in q space using the technique described here. A connection between $|\phi|$ and the $E(q)$ band dispersion has been made already [2, 13]

A.Mu. and J.E.O. are supported by the Universidad del País Vasco (9/UPV 00057.240-13668/2001) and the Max Planck Research Award Program. J.G.deA. acknowledges support by the Spanish Ministerio de Ciencia y Tecnología. F.J.H. acknowledges support by the NSF under Award Nos. DMR-9815416 and DMR-0084402.

[1] Ph. Avouris and I.-W. Lyo, Science **264**, 942 (1994).
[2] L. Bürgi, O. Jeandupeux, A. Hirstein, H. Brune, and K. Kern, Phys. Rev. Lett. **81**, 5370 (1998).
[3] R. K. Kawakami, E. Rotenberg, H. J. Choi, E. J. Escorcia-Aparicio, M. O. Bowen, J. H. Wolfe, E. Arenholz, Z. D. Zhang, N. V. Smith, Z. Q. Qiu, Nature **398**, 132 (1999).
[4] A. Mugarza, A. Mascaraque, V. Prez-Dieste, V. Repain, S. Rousset, F. J. Garca de Abajo, J. E. Ortega, Phys. Rev. Lett. **87**, 107601 (2001).
[5] S. Kono, C. S. Fadley, N. F. T. Hall, and Z. Hussain, Phys. Rev. Lett. **41**, 117 (1978).
[6] F. J. García de Abajo, M. A. Van Hove, and C. S. Fadley, Phys. Rev. B **63**, 75404 (2001).
[7] R. Otero, A. L. Vázquez de Parga, and R. Miranda, Surf. Sci. **447**, 143 (2000).
[8] D. K. Saldin, R. J. Harder, V. L. Shneerson, and W. Moritz, J. Phys.: Condens. Matter **13**, 10689 (2001).
[9] J. Miao, P. Charalambous, J. Kirz, and D. Sayre, Nature **400**, 342 (1999); J. Miao, D. Sayre, and H. N. Chapman, J. Opt. Soc. Am. A **15**, 1662 (1998).
[10] A. Mugarza *et al.*, Phys. Rev. B (submitted).
[11] The approximation of a factorized wave function is reasonable for states that are confined to a single terrace island. It breaks down for a superlattice with strong overlap between adjacent terraces where ϕ delocalized and discrete states become bands.
[12] M. Henzler, Appl. Phys. **9**, 11 (1976).
[13] J. I. Pascual, Z. Song, J. J. Jackiw, K. Horn, and H.-P. Rust Phys. Rev. B **63**, 241103 (2001).

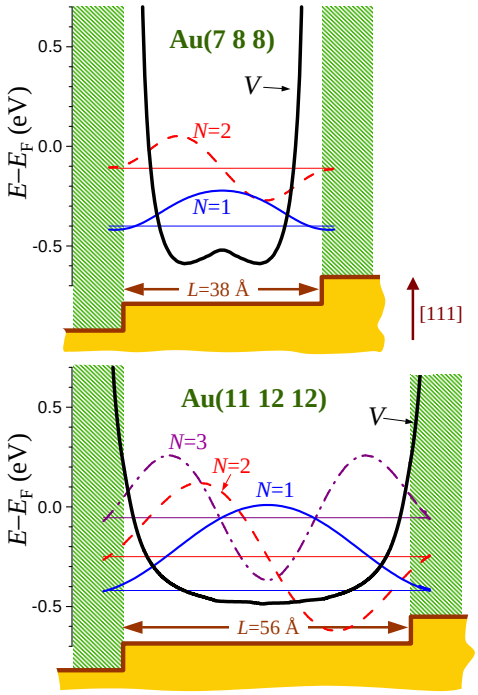

FIG. 1: Vicinal Au(111) surfaces with quantum well states confined by step edges. The energy levels are directly measured by angle-resolved photoemission. The confining potential V and the wave functions of states N=1,2,3 are obtained from the momentum distribution of the photoemission intensity.

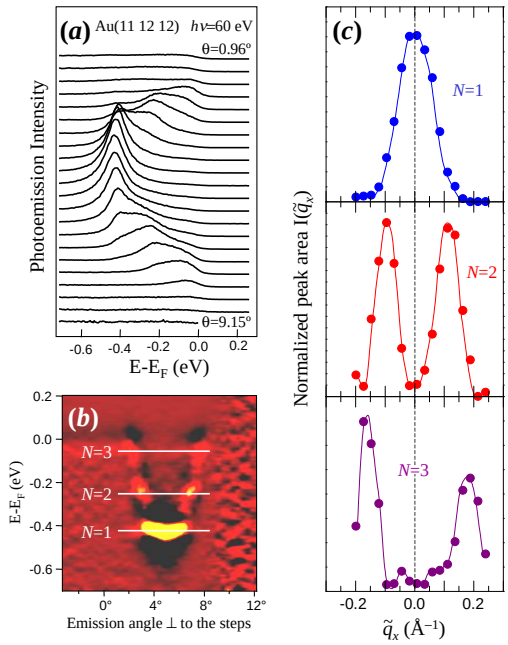

FIG. 2: **(a)** Photoemission spectra from Au(11,12,12) showing one-dimensional surface states. **(b)** Second energy derivative of the intensity showing the presence of three quantum levels E_N^{exp}. **(c)** Peak area of each quantum level obtained by line fitting of individual spectra in (a). The lines are spline-fits to the data points.

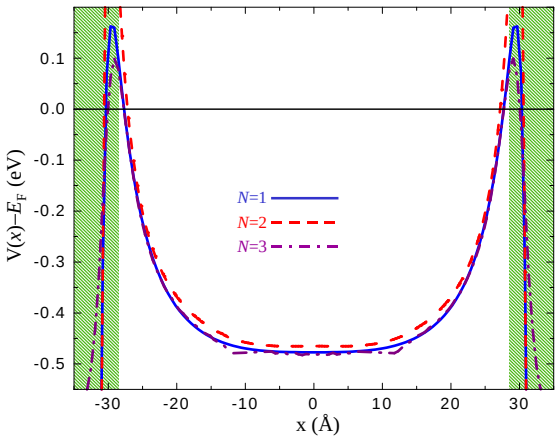

FIG. 3: Confining potentials V obtained from the experimental photoemission intensities of Fig. 2 for the N=1,2,3 states in Au(11,12,12) using the oversampling method.